

## Improved biocatalysts from a synthetic circular permutation library of the flavin-dependent oxidoreductase Old Yellow Enzyme.

Ashley B. Daugherty, Sridhar Govindarajan, and Stefan Lutz

*J. Am. Chem. Soc.*, **Just Accepted Manuscript** • DOI: 10.1021/ja4074886 • Publication Date (Web): 29 Aug 2013

Downloaded from <http://pubs.acs.org> on September 10, 2013

### Just Accepted

“Just Accepted” manuscripts have been peer-reviewed and accepted for publication. They are posted online prior to technical editing, formatting for publication and author proofing. The American Chemical Society provides “Just Accepted” as a free service to the research community to expedite the dissemination of scientific material as soon as possible after acceptance. “Just Accepted” manuscripts appear in full in PDF format accompanied by an HTML abstract. “Just Accepted” manuscripts have been fully peer reviewed, but should not be considered the official version of record. They are accessible to all readers and citable by the Digital Object Identifier (DOI®). “Just Accepted” is an optional service offered to authors. Therefore, the “Just Accepted” Web site may not include all articles that will be published in the journal. After a manuscript is technically edited and formatted, it will be removed from the “Just Accepted” Web site and published as an ASAP article. Note that technical editing may introduce minor changes to the manuscript text and/or graphics which could affect content, and all legal disclaimers and ethical guidelines that apply to the journal pertain. ACS cannot be held responsible for errors or consequences arising from the use of information contained in these “Just Accepted” manuscripts.



1  
2  
3  
4  
5  
6 **Improved biocatalysts from a synthetic circular permutation library of the**  
7  
8 **flavin-dependent oxidoreductase Old Yellow Enzyme.**  
9

10  
11  
12  
13 Ashley B. Daugherty<sup>§</sup>, Sridhar Govindarajan<sup>¶</sup>, Stefan Lutz<sup>§\*</sup>.  
14  
15

16  
17 § Department of Chemistry, Emory University, 1515 Dickey Drive, Atlanta, GA 30084, USA; ¶ DNA2.0,  
18 1140A O'Brian Drive, Menlo Park, CA 94025, USA.  
19  
20  
21  
22  
23  
24  
25  
26  
27  
28  
29  
30  
31  
32  
33  
34  
35  
36  
37  
38  
39  
40  
41  
42  
43  
44  
45  
46  
47  
48  
49  
50  
51  
52  
53  
54  
55  
56  
57  
58  
59  
60

**ABSTRACT**

Members of the the Old Yellow Enzyme (OYE) family are widely-used, effective biocatalysts for the stereoselective trans-hydrogenation of activated alkenes. To further expand their substrate scope and improve catalytic performance, we have applied a protein engineering strategy called circular permutation (CP) to enhance the function of OYE1 from *Saccharomyces pastorianus*. CP can influence a biocatalyst's function by altering protein backbone flexibility and active site accessibility, both critical performance features as the catalytic cycle for OYE1 is thought to involve rate-limiting conformational changes. To explore the impact of CP throughout the OYE1 protein sequence, we implemented a highly efficient approach for cell-free cpOYE library preparation by combining whole-gene synthesis with *in vitro* transcription/translation. The versatility of such an *ex vivo* system was further demonstrated by the rapid and reliable functional evaluation of library members under variable environmental conditions with three reference substrates ketoisophorone, cinnamaldehyde and (*S*)-carvone. Library analysis identified over 70 functional OYE1 variants with several biocatalysts exhibiting over an order of magnitude improved catalytic activity. Although catalytic gains of individual cpOYE library members vary by substrate, the locations of new protein termini in functional variants for all tested substrates fall within the same four distinct loop/lid regions near the active site. Our findings demonstrate the importance of these structural elements in enzyme function and support the hypothesis of conformational flexibility as a limiting factor for catalysis in wild type OYE.

## INTRODUCTION

The reduction of alkenes is a widely used and effective strategy for the asymmetric synthesis of chiral building blocks. While traditional catalysts for these reactions include chiral transition metal complexes<sup>1-3</sup> and organocatalysts<sup>4</sup>, enzymes offer a highly selective, evolvable and sustainable alternative.<sup>5-7</sup> More specifically, ene-reductases of the Old Yellow Enzyme (OYE) family [EC 1.3.1.31] are known to catalyze the highly stereoselective trans-hydrogenation of  $\alpha,\beta$ -unsaturated aldehydes, ketones, carboxylates, nitriles and nitroalkenes.<sup>8-14</sup> The redox chemistry of OYEs is facilitated by a non-covalently bound flavin mononucleotide (FMN) cofactor. Following reduction of the alkene substrate, the FMN is regenerated via hydride transfer from NADPH (Scheme 1).

The popularity of OYEs in biotechnological and pharmaceutical applications has resulted in the isolation and characterization of family members from a variety of organisms, providing a rich source of oxidoreductases for the conversion of alkenes.<sup>10,12,13,15-19</sup> At the same time, these biocatalysts represent attractive targets for protein engineers to further improve and customize their functional performances. A number of structure-guided site-directed and site-saturation mutagenesis studies, as well as directed evolution experiments have yielded OYE variants with improved catalytic properties including enhanced turnover rates, reversed enantioselectivity and increased stability.<sup>20-25</sup> Unfortunately, the reported gains in catalytic activity were generally modest (two to four-fold) although potential benefits of amino acid substitution in OYE family members are possible as demonstrated by the complete reversal of enantioselectivity as a result of a single amino acid change.<sup>23</sup> A review of past OYE engineering studies also identified a major experimental challenge. Following standard heterologous expression of OYEs in *Escherichia coli* (*E. coli*), the functional characterization of the exogenous oxidoreductase is complicated by the host's endogenous reductase activity, hence requiring additional purification steps prior to functional evaluation.<sup>20</sup> Consequently, library analysis has typically been limited to either small numbers of variants or to substrates with low background from host reductases.<sup>22,23</sup> Future efforts involving larger,

1  
2  
3 more comprehensive protein libraries for tailoring OYE family members would clearly benefit from a  
4  
5 more effective library preparation and analysis protocol.  
6

7  
8 Our OYE engineering efforts were motivated by a number of biochemical studies and  
9  
10 crystallographic structure analyses that suggested substantial conformational changes as part of the  
11  
12 enzyme's catalytic cycle. Spectroscopic evidence for such conformational changes in kinetic  
13  
14 measurements and structural differences in crystals of apo-form and substrate-bound OYEs, as well as  
15  
16 more recent data from an engineering study of *Zymomonas mobilis* NCR enoate reductase all support the  
17  
18 hypothesis that structural rearrangements of loops and domains play an important and possibly rate-  
19  
20 limiting role in the catalytic function of these enzymes.<sup>25-31</sup> We therefore decided to test the functional  
21  
22 role of various flexible regions in OYE1 from *Saccharomyces pastorianus* (formerly *S. carlsbergensis*),  
23  
24 the most extensively studied member of the OYE family, by a protein engineering strategy called circular  
25  
26 permutation (CP). During CP, a protein's original amino and carboxyl-termini are covalently linked by a  
27  
28 peptide linker and new termini are introduced elsewhere in the protein structure through the breakage of a  
29  
30 peptide bond.<sup>32</sup> While such termini relocation leaves the amino acid composition of the protein  
31  
32 unchanged, the sequence reorganization has been shown to affect a protein's local conformational  
33  
34 flexibility. For new termini positioned near an enzyme active site, the altered protein dynamics can  
35  
36 significantly impact catalytic performance by translating into greater active site accessibility and  
37  
38 modifying rate-determining structural changes.<sup>33-38</sup>  
39  
40  
41

42 Here, we report on the identification and characterization of catalytically improved OYE1  
43  
44 variants via CP. To address the aforementioned practical limitations for working with combinatorial  
45  
46 libraries of OYE, we have opted for a whole-gene synthesis approach which gives access to an idealized  
47  
48 gene library with maximal (theoretical) diversity at minimal size. Subsequent synthesis of the  
49  
50 corresponding cpOYE variants is accomplished via *in vitro* transcription/translation (IVTT) using the  
51  
52 chemically defined PURE system which almost completely eliminates background reductase activity.<sup>39,40</sup>  
53  
54 This *ex vivo* protein engineering strategy has proved highly effective for the parallel synthesis of hundreds  
55  
56 of OYE library members whose catalytic activity can be assessed without further need for purification.  
57  
58  
59  
60

1  
2  
3 The evaluation of our new protocol for OYE1 library screening on three reference substrates is described.  
4  
5 The approach has helped to identify a number of candidates with significantly (>10-fold) enhanced  
6  
7 catalytic performance. Evidence in support of the critical role of loop and domains near the active site are  
8  
9 found in the systematic analysis of protein variants with multiple substrates and detailed characterization  
10  
11 of selected cpOYE variants.  
12  
13

## 14 15 16 17 18 MATERIAL AND METHODS 19

20  
21  
22  
23 **Materials.** Whole-gene synthesis was performed by DNA2.0 (Menlo Park, CA). PURExpress kits were  
24  
25 purchased from New England Biolabs (Ipswich, MA). All reagents, substrates, and reference materials  
26  
27 were obtained from Sigma-Aldrich (St. Louis, MO) unless otherwise indicated.  
28  
29

30  
31 **cpOYE1 library synthesis.** The gene encoding OYE1 from *S. pastorianus* (formerly *S. carlsbergensis*;  
32  
33 NCBI access number: X53597.1) served as starting sequence for our experiments. The CP library was  
34  
35 prepared by PCR amplification of gene sequences encoding the individual variants using an *oye1* tandem  
36  
37 repeat as template (Fig. 1). The tandem repeat was created by whole-gene synthesis, linking two copies of  
38  
39 *oye1* head-to-tail via an oligonucleotide sequence encoding a three amino acid linker (-Gly-Ser-Thr-). The  
40  
41 Start and Stop codons of the 399-amino acid enzyme were eliminated in the tandem repeat. Subsequently,  
42  
43 gene sequences corresponding to individual circular permuted enzymes were obtained by PCR  
44  
45 amplification using the tandem repeat as template in combination with sequence-specific oligonucleotide  
46  
47 primers. In the 5'-regions of the forward primers, a ATG start codon was included while reverse primers  
48  
49 carried a TAA termination codon. The PCR products were subcloned into pET-14b (Novagen) via  
50  
51 flanking type-IIs restriction endonuclease cleavage sites (*BsaI*) to enable ligation of PCR products into the  
52  
53 vector's *NcoI/XhoI* sites independent of variations in the *oye1* library sequences. Following  
54  
55 transformation of individual ligation reactions into *E. coli*, plasmid DNA from selected colonies was  
56  
57  
58  
59  
60

1  
2  
3 extracted and gene sequences were verified by DNA sequencing. Aliquots of confirmed plasmids carrying  
4 specific library members were stored separately in 96-well microtiter plates.  
5  
6  
7

8  
9  
10 **Primary library screening.** All members of the cpOYE library were initially evaluated for catalytic  
11 function by *in vitro* transcription/translation (IVTT) followed by an *in situ* ene-reductase activity assay.  
12 Overall, the IVTT reactions were assembled using the PURExpress *in vitro* protein synthesis kit (PURE)  
13 following manufactures protocol with a few adjustments (see below) optimized for our application.  
14 Reactions were assembled in a 96-well microtiter plate on a 10- $\mu$ L scale containing PURExpress solution  
15 A, PURExpress solution B, 100  $\mu$ M FMN, 10 units RNase Inhibitor (NEB), 100 ng DNA template, and  
16 nuclease-free H<sub>2</sub>O. All reactions from the cpOYE library screening were ran simultaneously with wild  
17 type OYE1 (positive control) and dihydrofolate reductase (DHFR; negative control; provided with the  
18 PURExpress kit) under the same experimental conditions. The reactions were incubated at 37°C for 2.5 h  
19 to allow for adequate protein synthesis prior to the activity assay. The reactions were cooled to 4°C to  
20 stop the reaction. Subsequently, ene-reductase activity was assessed under anaerobic conditions (Coy  
21 Laboratory Products, Grass Lake, MI) at ambient temperature utilizing glucose dehydrogenase (GDH)  
22 from *Thermoplasma acidophilum* for NADPH regeneration. The IVTT reaction was mixed with substrate  
23 (200  $\mu$ M ketoisophorone (**1**), 200  $\mu$ M cinnamaldehyde (**3**), or 1 mM *S*-carvone (**5**)), 200  $\mu$ M NADP<sup>+</sup>, 2 U  
24 GDH, and 100 mM glucose. The 30- $\mu$ L assay ran for 2.5 h (due to high turnover, reaction time for **3** was  
25 reduced to 30 min) and was quenched by mixing with an equal amount of ethyl acetate containing 1 mM  
26 cyclohexanone as internal standard. A sample of the organic phase was injected on an Agilent  
27 technologies 6850 GC machine equipped with a chiral CycloSil-B column (30 m x 0,32 mm / 0.25  $\mu$ m,  
28 Agilent, Santa Clara, CA) using hydrogen as the carrier gas (flow rate 1.8 mL/min) and an FID detector  
29 (detector temperature 200°C, split ratio 25:1). The temperature program for **1** - **4**: 150°C hold 10 min.  
30 (Retention time: **1** = 3.54 min; **2** = 3.86 min (*R*-isomer); 3.95 min (*S*-isomer), **3** = 6.1 min, **4** = 3.64 min.  
31 For **5** and **6**: 90°C hold 5 min, then 1°C/min to 120°C (Retention times: **5** = 27.54 min; **6** = 23.1 min  
32 (1*R*/4*S*-isomer); 22.92 min (1*S*/4*S*-isomer). The percent conversions and enantiomeric excess was  
33  
34  
35  
36  
37  
38  
39  
40  
41  
42  
43  
44  
45  
46  
47  
48  
49  
50  
51  
52  
53  
54  
55  
56  
57  
58  
59  
60

1  
2  
3 calculated from substrate and product integration areas and were quantified using standard curves  
4  
5 generated using known amounts of the substrate and product.  
6  
7

8  
9  
10 **Protein expression and purification.** Selected members of the cpOYE library were chosen for a more  
11 detailed *in vitro* characterization in order to confirm and further characterize interesting variants from the  
12 primary library screening analysis. Individual plasmid DNA encoding the corresponding library members  
13 was initially transformed in *E. coli* BL21(DE3)pLysS for expression. Colonies were cultured in 2 mL LB  
14 medium containing chloramphenicol (34 µg/ml) and ampicillin (100 µg/ml) overnight at 37°C. The  
15 overnight culture was used to inoculate 2YT medium containing the same antibiotics and cultures were  
16 grown at 37°C until the OD(600) reached 0.5 to 0.7. Overexpression was induced by addition of IPTG to  
17 a final concentration of 0.4 mM and cultures were overexpressed for 18 h at 20°C. Subsequently, cultures  
18 were centrifuged for 20 min at 4°C and 4000g and cell pellets were stored at -20°C until purification. The  
19 purification of wild type OYE1 and variants followed the same purification procedure. Cell pellets from a  
20 250 mL culture was resuspended in 6 mL of buffer A (40 mM Tris-HCl (pH 8.0), 20 mM NaCl). To the  
21 mixture, 75 µL of protease inhibitor cocktail (Sigma), 7.5 µL of benzonase (Novagen), and 10 µM PMSF  
22 were added and stored on ice for 30 min. Cells were lysed using sonication (8x with 10 sec pulses and 20  
23 sec pauses). After centrifugation for 30 min at 4°C and 10,000g, the clear lysate was further purified via  
24 anion-exchange chromatography (HiTrap Q HP-5mL column pre-equilibrated with buffer A). The column  
25 was washed with 2 column volumes (CV) of buffer A, followed by a linear gradient to 100% buffer B (40  
26 mM Tris-HCl (pH 8.0), 1 M NaCl) over 10 CV. Product fractions were combined and concentrated to ~1  
27 mL using a Millipore filter unit (MWCO: 10 kDa). In a final polishing step, proteins were purified by size  
28 exclusion chromatography (Superdex 200, 10/300 GL column equilibrated with buffer C (40 mM Tris-  
29 HCl (pH 8.0), 300 mM NaCl); flow rate: 0.5 mL/min). Elution of protein was monitored by UV-detection  
30 at 280 nm and 460 nm and product fractions were combined. SDS-PAGE analysis of the final product  
31 showed >95% purity.  
32  
33  
34  
35  
36  
37  
38  
39  
40  
41  
42  
43  
44  
45  
46  
47  
48  
49  
50  
51  
52  
53  
54  
55  
56  
57  
58  
59  
60

1  
2  
3 **Spectral properties of OYE1 variants.** All spectral analysis of OYE1 and permutants was completed  
4 using a Varian Cary 100 spectrophotometer. The extinction coefficient for each variant was determined  
5 by recording the absorbance spectrum of the protein-bound FMN solution in 10 mM Tris-HCl (pH 7.5)  
6 buffer. A 25  $\mu$ L aliquot of 10% SDS was added to denature the protein and spectra were recorded until  
7 changes were no longer observed. The extinction coefficient for each enzyme-bound FMN was calculated  
8 using the following equation:  $\epsilon = \epsilon_{\text{free(FMN)}} (12,500 \text{ M}^{-1}\text{cm}^{-1}) \times (\text{absorbance (at } \lambda_{\text{max}}) \text{ of FMN}_{\text{bound}} \text{ (prior to}$   
9  $\text{SDS treatment) / absorbance (at } \lambda_{\text{max}}) \text{ of FMN}_{\text{bound}} \text{ (after SDS))}$ .<sup>41</sup>  
10  
11  
12  
13  
14  
15  
16  
17

18 Phenolate inhibitor binding assays were completed at room temperature in 100 mM potassium  
19 phosphate buffer pH 7 using a cuvette with a 1-cm path length (Fig. S1) The initial enzyme concentration  
20 (10-30  $\mu$ M) in each experiment was calculated by the corresponding FMN extinction coefficient. Aliquots  
21 of *p*-hydroxybenzaldehyde were added to the protein solution and spectra were recorded after 3 min of  
22 equilibration until apparent saturation was reached. The long wavelength charge transfer maximum values  
23 for each data set were determined by first derivative analysis and extinction coefficients were calculated  
24 based on the absorbance values (Table 2). Separately, dissociation constants were calculated by plotting  
25  $[\text{ligand}]_{\text{free}}$  versus Y (fractional saturation of OYE) and analysis by non-linear curve fit using GraphPad  
26 Prism6 (GraphPad, La Jolla, CA) (Fig.S1 inserts).  
27  
28  
29  
30  
31  
32  
33  
34  
35  
36  
37  
38  
39

40 **Activity assays.** The enzyme concentration for each cpOYE variant was determined based on the  
41 extinction coefficient of protein-bound FMN. Purified enzyme was assayed in an anaerobic chamber (Coy  
42 LabProducts) by incubating 0.1-1  $\mu$ M enzyme with 1 mM **1**, 200  $\mu$ M NADP<sup>+</sup>, 5 U GDH, 100 mM  
43 glucose in 500- $\mu$ L total reaction volume. The reaction was monitored over 45 min (timed to achieve less  
44 than 30% product formation) by taking aliquots and mixing with an equal amount of ethyl acetate and  
45 analyzed via GC (see above). The product was quantified using a standard curve generated using known  
46 amounts of the product (*R*)-levodione (**2**) and 1 mM cyclohexanone as internal standard. Alternatively,  
47 turnover was monitored spectrophotometrically at ambient temperatures with the Bioteck EPOCH plate  
48 reader housed in the anaerobic chamber. Purified enzyme was assayed following the decrease in  
49  
50  
51  
52  
53  
54  
55  
56  
57  
58  
59  
60

1  
2  
3 absorbance of NADPH at 340 nm (molar extinction coefficient  $6,220 \text{ M}^{-1}\text{cm}^{-1}$ ). The 300- $\mu\text{L}$  reaction  
4 contained 100 mM sodium phosphate buffer (pH 7.0), 1 mM of the appropriate substrate (from 20 mM  
5 stock in ethanol), 100  $\mu\text{M}$  NADPH and 0.1-1  $\mu\text{M}$  enzyme. For **3**, where substrate saturation was not a  
6 problem, kinetic constants were determined by fitting initial rates to the Michaelis-Menten equation  
7 through a non-linear curve fit using Origin7 (OriginLab, Northampton, MA) (Table S1). The  
8 stereoselectivity displayed by the permutants for reducing (*S*)-**5** was determined by incubating 25  $\mu\text{g}$   
9 enzyme with 5 mM substrate, 200  $\mu\text{M}$  NADP<sup>+</sup>, 5 U GDH, and 100 mM glucose in 500- $\mu\text{L}$  total reaction  
10 volume. The reaction was carried out for 24 h at room temperature. After quenching, the reaction was  
11 extracted with an equal amount of ethyl acetate and the organic layer analyzed by chiral GC.  
12  
13  
14  
15  
16  
17  
18  
19  
20  
21  
22  
23  
24

25 **Stopped flow experiments.** Measurements were made on an OLIS RSM-1000 (Olis Inc., Bogart, GA)  
26 stopped flow spectrophotometer under anaerobic conditions in 50 mM Tris-HCl (pH 7.5) at 25 °C. For  
27 the reductive half reaction, OYE1 or cpOYE303 (10  $\mu\text{M}$ ) were mixed in the spectrophotometer with  
28 NADPH (final concentration: 50 - 500  $\mu\text{M}$ ). The oxidative half reaction was studied with **1** as substrate.  
29 Enzyme (13  $\mu\text{M}$ ) was preincubated with 20  $\mu\text{M}$  NADPH to completely reduce FMN, followed by mixing  
30 with **1** (0.25 mM and 0.5 mM for OYE1; 0.5 mM and 1 mM for cpOYE303). Spectra were recorded with  
31 delays of 10 sec and 100 sec after mixing. All data analysis was performed in GraphPad Prism 6  
32 (GraphPad, La Jolla, CA).  
33  
34  
35  
36  
37  
38  
39  
40  
41  
42  
43  
44  
45

## 46 RESULTS AND DISCUSSION

47  
48  
49  
50

51 The structurally and functionally well-characterized OYE1 from *S. pastorianus* was chosen to test  
52 our hypothesis that CP of an OYE family member could yield variants with improved catalytic  
53 performance. Initially, we analyzed representative structures of OYE1 (PDB access code: 1OYA<sup>30</sup> and  
54 1K03<sup>26</sup>) to determine a suitable linker sequence for connecting the native amino and carboxyl termini.  
55  
56  
57  
58  
59  
60

1  
2  
3 Trimming the C-terminus by three residues shortened the termini distance from 13Å to 6Å without  
4 impacting the catalytic performance of the wild type enzyme. The remaining (shorter) gap was bridged by  
5 a flexible, hydrophilic three-amino acid residue linker (-Gly-Thr-Ser-).  
6  
7  
8

9  
10 Taking advantage of whole-gene synthesis, we abandoned the previously employed random  
11 circular permutation protocol<sup>33,42</sup> to instead prepare a fully synthetic DNA library of circular permuted  
12 OYE1 (cpOYE) variants. A tandem-OYE1 gene sequence was prepared by chemical DNA synthesis that  
13 served as template for PCR amplification of individual cpOYE variants (Fig. 1). This strategy  
14 dramatically reduces the size of the circular permutation library by eliminating out-of-frame and inversely  
15 cloned representatives in the sequence pool. Furthermore, parallel cloning of individual genes into an  
16 appropriate DNA vector for protein expression, followed by verification of the correct DNA sequence for  
17 each library member creates a chemically defined collection of enzyme variants. Such up-front efforts  
18 during library generation is advantageous as it dramatically simplifies library analysis by eliminating the  
19 need for oversampling. For practical reasons, we created a focused cpOYE library by synthesizing only  
20 every other possible variant, starting with even-numbered positions at the N-terminus of OYE1. In  
21 addition, variants within  $\pm 6$  amino acids to the native termini were left out as they are predicted to at best  
22 show wild type-like activity. Following the initial functional evaluation of this primary library, odd-  
23 numbered variants in regions of interest were quickly prepared by the same PCR-based method. Over the  
24 course of this entire study, we synthesized and screened a total of 228 cpOYE variants, identifying  
25 roughly 70 members (~30%) in our circular permutation library with equal or better than wild type  
26 activity for reduction of ketoisophorone (**1**), a widely used reference substrate for the functional  
27 evaluation of OYE family members (see below).  
28  
29  
30  
31  
32  
33  
34  
35  
36  
37  
38  
39  
40  
41  
42  
43  
44  
45  
46  
47

48 Building on the idea of a synthetic protein engineering approach, we employed the PURE system  
49 for functional analysis of the cpOYE library. PURE distinguishes itself from other IVTT systems in that  
50 all of its components are isolated and purified individually, followed by reconstitution of a chemically  
51 fully defined functional protein synthesis machinery.<sup>39,40</sup> As such, PURE dramatically lowers the  
52 background signal caused by contaminating endogenous reductases in cell-based *in vitro* and *in vivo*  
53  
54  
55  
56  
57  
58  
59  
60

1  
2  
3 expression systems and allows for direct assaying of enzyme activity (Fig. S2). Furthermore, PURE is  
4 highly scalable and allows for parallel synthesis of library members in 96-well microtiterplate format with  
5 relatively consistent protein yields ( $\pm 50\%$  based on SDS-PAGE analysis; data not shown). In subsequent  
6 activity assays, a 10- $\mu\text{L}$  PURE reaction produced enough enzyme ( $\sim 0.1 \mu\text{M}$ ) for detecting reduction of **1**  
7 by OYE1 variants with as little as 10% of wild type activity. Activity assays performed under anaerobic  
8 conditions maximize the signal-to-noise ratio, presumably eliminating side reactions and enzyme  
9 inactivation by reactive oxygen species generated in the presence of reduced FMN.<sup>20</sup> Finally, expression  
10 of catalytically competent OYE required supplementation of the IVTT reaction mixture with FMN.  
11 Maximum enzyme activity was reached at  $[\text{FMN}] > 1 \mu\text{M}$  which is approximately 100-fold above the  
12 reported dissociation constant for FMN in OYE1 (Fig. S3).<sup>43</sup> We further raised the  $[\text{FMN}]$  to 100  $\mu\text{M}$  to  
13 ensure saturation of enzyme with cofactor, even for engineered OYEs with potentially lower cofactor  
14 binding affinity.  
15  
16  
17  
18  
19  
20  
21  
22  
23  
24  
25  
26  
27  
28

29 Our initial functional evaluation of the cpOYE library focused on the stereoselective reduction of  
30 **1** to **R-2**, one of the most prominent industrial application for ene-reductases and a widely used standard  
31 for the functional evaluation of OYE family members.<sup>16,17,44-47</sup> Preliminary screening with PURE quickly  
32 identified  $\sim 70$  cpOYE variants with catalytic activity equal or better than wild type enzyme. The location  
33 of the new termini in these active variants fell into four distinct sectors within the primary sequence (Fig.  
34 2A). Sector I covers most of the exterior helical subdomain (amino acid residues 125-160; numbering  
35 based on OYE1) while sectors II and III include loop/helix regions 5 (residues 250-265) and 6 (residues  
36 290-310), respectively (Fig. 3). Sector IV represents a short loop (residues 375-380) near the native C-  
37 terminus. The activity assay suggested that permutants with new termini in sector III were particularly  
38 beneficial for effective reduction of **1**, showing  $>400\%$  of wild type activity for multiple cpOYE variants.  
39 Analysis of the reaction mixtures by chiral GC confirmed unchanged *R*-enantioselectivity for all active  
40 cpOYE variants with native-like  $ee_R$ -values of  $>98\%$ . From a practical perspective, we were interested in  
41 whether the observed activity differences in PURE were reliable predictors of catalytic activity measured  
42 with purified enzyme. To assess the predictability of activity in PURE, we selected nine cpOYE variants  
43  
44  
45  
46  
47  
48  
49  
50  
51  
52  
53  
54  
55  
56  
57  
58  
59  
60

1  
2  
3 (cpOYE146, 154, 160, 257, 260, 291, 292, 303, 306 and 378; the number indicates the location of a  
4 variant's new N-terminal based on the numbering of residues in wild type enzyme) which showed 1 to 4-  
5 fold activity gains over OYE1 in the PURE reactions with **1**. Enzyme samples of these nine CP variants  
6 and OYE1 were obtained through (traditional) heterologous expression and purification, followed by  
7 kinetic measurements of individual conversion rates for **1** (Table 1). Determination of the Michaelis-  
8 Menten parameters was not possible as enzyme saturation could not be reached due to limited solubility  
9 of **1**. The kinetic data showed rate increases by up to 19-fold (for cpOYE303) over wild type enzyme. The  
10 data also indicate that PURE systematically underestimates the rates compared to purified enzyme.  
11 Nevertheless, the observed changes in the IVTT system were overall proportional - the top performers in  
12 the PURE system also showed the highest catalytic gains with purified enzyme. These results suggest that  
13 the IVTT results are semi-quantitative and can be used as reliable predictors of enzyme activity.  
14  
15  
16  
17  
18  
19  
20  
21  
22  
23  
24  
25  
26

27 The experimental data for reduction of **1** led to three questions concerning the structure-function  
28 relationship in these engineered OYE variants: a.) will the same four sectors be identified upon screening  
29 with other substrates, b.) will sector III always be the preferred site for termini relocation, and c.) will  
30 native *R*-enantioselectivity be preserved for other substrates? We explored the first question by screening  
31 the cpOYE library for improvements in ene-reductase activity with cinnamaldehyde (**3**) and *S*-carvone (**5**)  
32 as substrates (Fig. 2B/C). Both compounds are important intermediates in the fragrance and flavor  
33 industry. Library screening with these two substrates identified functional variants in the same four  
34 sectors of the protein sequence. For conversion of **3**, the catalytic improvements upon CP appeared  
35 moderate, an observation that was confirmed in activity assays with purified enzyme which detected up to  
36 2-fold rate increases in catalytic efficiency for cpOYE260 (Table 1). We hypothesize that the already high  
37 catalytic efficiency of OYE1 for reduction of **3** makes it more likely for additional functional gains to be  
38 countered by undesirable structural perturbations upon CP. In contrast, the screening of our cpOYE  
39 library with **5** showed significant catalytic improvements for variants in all four sectors. These functional  
40 gains were independently verified in subsequent activity assays with purified enzyme, showing 3 to 13-  
41 fold increases in the rate of conversion (Table 1). As for **1**, the limited substrate solubility of **5** prevents  
42  
43  
44  
45  
46  
47  
48  
49  
50  
51  
52  
53  
54  
55  
56  
57  
58  
59  
60

1  
2  
3 the determination of detailed kinetic parameters and no changes in the native enzyme's *R*-selectivity for  
4 the conversion of *S*-**5** to *cis*-1*R*/4*S*-**6** were detected. Summarizing the screening results for **1**, **3** and **5**, all  
5 active candidates among the OYE1 variants had their new protein termini located in the same four  
6 sectors. The exclusivity of functional variants in these sectors might at least in part associated with  
7 protein foldability upon termini relocation. Nevertheless, their proximity to the active site and in some  
8 cases significant improvement in catalytic activity over the native enzyme suggests additional benefits  
9 arising from changes in conformational flexibility and active site accessibility. The same data also showed  
10 that relative catalytic performance of cpOYE variants differs with individual substrates. Although variants  
11 in sector III are clearly the best biocatalysts for **1**, sectors I and IV offer slight activity gains for **3** while  
12 variants from all four sectors show substantive functional benefits for reduction of **5**. The observed  
13 preference of the three substrates for protein termini in certain sectors and those sectors' location relative  
14 to the substrate binding site could provide clues to the underlying structure-function relationship. Future  
15 in-depth structure studies on selected cpOYE variants via x-ray crystallography will help to address these  
16 questions in more detail. In summary, the relocation of protein termini in OYE1 introduced structural and  
17 conformational changes in distinct portions of the active site, in turn affecting substrate binding affinity,  
18 orientation and catalytic turnover.

19  
20  
21  
22  
23  
24  
25  
26  
27  
28  
29  
30  
31  
32  
33  
34  
35  
36  
37  
38 To further investigate the nature of the catalytic rate enhancements, we conducted a series of  
39 rapid reaction kinetic experiments with wild type OYE1 and cpOYE303, the variant with the most  
40 significant functional improvements (Fig. 4). The enzyme's catalytic cycle can be split into two steps; a  
41 reductive half reaction representing the NADPH-driven reduction of the oxidized flavoprotein and an  
42 oxidative half reaction involving reoxidation of the reduced flavin cofactor upon substrate conversion  
43 (Scheme 1). Based on studies by Massey and coworkers, the reductive half reaction can be further divided  
44 into three sub-steps: i) initial binding of NADPH to enzyme (E)•FMN<sub>ox</sub> followed by ii) conformational  
45 changes and repositioning of the nicotinamide cofactor from E•FMN<sub>ox</sub>•NADPH to E\*•FMN<sub>ox</sub>•NADPH  
46 and finally iii) hydride transfer.<sup>29</sup> For wild type OYE1, formation of E•FMN<sub>ox</sub>•NADPH is observed in  
47 stopped-flow experiments as the adduct generates a short-lived charge-transfer complex with a  
48  
49  
50  
51  
52  
53  
54  
55  
56  
57  
58  
59  
60

1  
2  
3 characteristic red-shifted FMN absorption peak near 460 nm. Subsequent reorientation of the flavin  
4 (E\*•FMN<sub>ox</sub>•NADPH) and reduction of the flavin cofactor results in the disappearance of the 460-nm  
5 band. In agreement with Massey's data, we detected the intermediate in our reaction catalyzed by wild  
6 type OYE1, yet the global fit analysis of spectral data for the engineered variant cpOYE303 did not  
7 indicate accumulation of an observable charge-transfer complex prior to reduction (Fig. 4B). At the same  
8 time, the overall rates of the reductive half reaction for OYE1 ( $k_{\text{red}} = 5.1 \pm 0.2 \text{ s}^{-1}$ ) and cpOYE303 ( $k_{\text{red}} =$   
9  $5.4 \pm 0.2 \text{ s}^{-1}$ ) remained largely unchanged (Fig. 4C). Given these observations, we rationalized the  
10 absence of an intermediate in cpOYE303 with an increased dissociation rate for NADPH from  
11 E•FMN<sub>ox</sub>•NADPH. Such an explanation is also consistent with previous reports from structural studies  
12 that emphasized the importance of conformational changes in loop region 5 (amino acid positions 290-  
13 310) as part of the reductive half reaction.<sup>31</sup> The location of the new protein termini in cpOYE303 in this  
14 region is likely responsible for the lower NADPH binding affinity, reflecting the increased local  
15 conformational flexibility upon cleavage of the polypeptide sequence which has been observed in  
16 numerous structure studies with circularly permuted proteins.<sup>35,48-51</sup> In summary, protein sequence  
17 reorganization by CP does impact the NADPH binding step of the reductive half reaction but at least in  
18 the case of cpOYE303 leaves the overall rate of the reductive half reaction unchanged.

19  
20  
21  
22  
23  
24  
25  
26  
27  
28  
29  
30  
31  
32  
33  
34  
35  
36  
37  
38 In contrast, the observed rate for the oxidative half reaction increases significantly upon CP and  
39 largely accounts for the gains in catalytic activity measured by steady-state kinetics. Following pre-  
40 incubation of the two OYEs with NADPH to fully reduce the enzyme-bound FMN, the rates of cofactor  
41 reoxidation ( $k_{\text{ox}}$ ) were measured after mixing with **1** (Fig. 4D). For both enzymes, the data could be fitted  
42 to a single-exponential function, yielding initial rates of conversion for cpOYE303 and OYE1 of  $0.63 \pm$   
43  $0.09 \text{ s}^{-1}$  and  $0.06 \pm 0.01 \text{ s}^{-1}$ , respectively. The data indicate that FMN reoxidation with **1** is significantly  
44 slower than cofactor reduction in both OYEs and likely represents the rate-limiting step in the reaction  
45 cycle. More importantly, we observe an eleven-fold rate increase for cpOYE303 over OYE1 which  
46 accounts for most of the gains in catalytic activity observed for the OYE variant in our steady-state  
47 kinetic measurements (Table 1). Although these initial studies do not reveal detailed information  
48  
49  
50  
51  
52  
53  
54  
55  
56  
57  
58  
59  
60

1  
2  
3 regarding the effects of CP on the individual steps along the reaction coordinate, the results clearly show  
4 that rate enhancement in the OYE-catalyzed reduction of **1** by cpOYE303 is due to changes in the  
5 oxidative half reaction. However, it seems unlikely that the observed functional effect is general. Previous  
6 studies have shown that the nature of the rate-limiting step in OYE can change as a function of  
7 substrate.<sup>28,29</sup> While we believe that the catalytic gains measured for the reduction of *S*-(**5**) originate from  
8 similar beneficial effects on the oxidative half reaction, the lack of change for **3** could be explained by  
9 differences in the rate-determining step.  
10  
11

12  
13  
14  
15  
16  
17  
18 In the absence of detailed crystallographic information, we investigated perturbations of the  
19 active site environment as a result of CP via changes in the spectral properties of the flavin cofactor. Upon  
20 binding of *p*-hydroxybenzaldehyde to OYE1, Massey and coworkers observed distinct long wavelength  
21 charge-transfer bands ranging from 560 to 590 nm with  $\lambda_{\text{max}}$  values depending on hydrogen-bonding  
22 interactions of the phenolate and the FMN redox potential.<sup>43,52</sup> The spectral properties of cpOYE variants  
23 can therefore serve as sensitive probes for the active site environment. Our analysis of representative  
24 variants from all four sectors with *p*-hydroxybenzaldehyde did indicate subtle but significant active site  
25 changes (Table 2 & Fig. S1). While small, two-fold differences in dissociation constants for the phenolate  
26 are consistent with overall integrity of the active site binding pocket, the shifts in  $\lambda_{\text{max}}$  values of the  
27 charge-transfer bands from 564 nm to 582 nm (relative to 578 nm for wild type OYE1) reflect changes in  
28 the FMN redox potential of ~20 mV which suggest small conformational and environmental perturbations  
29 near the cofactor. Nevertheless, the change in redox potentials for the cpOYE variants did not show a  
30 clear correlation with catalytic activity for our three substrates.  
31  
32  
33  
34  
35  
36  
37  
38  
39  
40  
41  
42  
43  
44  
45  
46  
47  
48  
49  
50

## 51 CONCLUSIONS

52  
53  
54

55 We have identified a series of circularly permuted OYE variants with enhanced ene-reductase  
56 activity for two representative enones and an enal. For all three substrates, the new protein termini of  
57  
58  
59  
60

1  
2  
3 catalytically active and improved enzymes fall in the same four structural regions including three loops  
4 and a helical subdomain near the active site. The functional benefits of new termini in these regions  
5 varied with substrate, presumably reflecting subtle differences in protein structure and interaction with the  
6 substrates. The native enzyme's high enantioselectivity was preserved in all cpOYE variants and catalytic  
7 activity for **1** and *S*-**5** was improved by >10-fold. The rapid reaction kinetics analysis of the oxidative and  
8 reductive half reactions in wild type OYE1 and cpOYE303 suggests that the functional gains can almost  
9 exclusively be attributed to improvements of the rate-limiting oxidative half reaction with **1**. Further in-  
10 depth studies of the individual steps in the reaction cycle will be required to explore whether the observed  
11 rate enhancements are more specifically due to changes in binding of **1**, release of (*R*)-**2**, or the catalytic  
12 step. Initial evidence in support of beneficial changes to substrate/product affinity upon CP was found in  
13 the absence of the characteristic charge-transfer complex ( $E \cdot FMN_{ox} \cdot NADPH$ ) in the reductive half  
14 reaction of cpOYE303. The accumulation of the complex in wild type OYE1 has been associated with a  
15 required conformational change involving loop 5; the same loop where the new protein termini in  
16 cpOYE303 are located. The increased conformational flexibility of a protein's termini region is well  
17 established in the literature and could explain the improved catalytic activity in our engineered OYE  
18 variants. Crystallographic and in-depth biophysical studies will help to further rationalize the observed  
19 differences in catalytic performance. Beyond the exploration of fundamental aspects of enzyme catalysis,  
20 our results demonstrate that CP offers an effective strategy for improving the catalytic performance of  
21 OYE1. Although a direct comparison with other mutagenesis-based engineering approaches is  
22 complicated by differences in reaction conditions and substrates, the rate enhancements for our cpOYE  
23 variants are of similar magnitude or better than for previously reported OYE variants.<sup>22,53</sup> For future  
24 experiments, the structural and functional similarities among enzymes of the OYE family suggests that  
25 CP could result in similar functional gains in other family members. Furthermore, selected cpOYE  
26 variants do not necessarily mark the end point of a protein engineering project but can serve as novel  
27 templates for subsequent mutagenesis experiments, allowing for even greater diversity in tailoring these  
28 biocatalysts to specific conditions and substrates. On the technical side, the use of a chemically defined  
29  
30  
31  
32  
33  
34  
35  
36  
37  
38  
39  
40  
41  
42  
43  
44  
45  
46  
47  
48  
49  
50  
51  
52  
53  
54  
55  
56  
57  
58  
59  
60

1  
2  
3 cpOYE gene library in combination with the PURE system dramatically accelerated the process of  
4  
5 identifying catalytically improved cpOYE variants for any substrate of choice. As technological advances  
6  
7 continue to raise efficacy and lower costs, we envision such synthetic protein engineering approaches to  
8  
9 become a popular new tool for synthetic biologists. For engineering OYE and cofactor-dependent  
10  
11 enzymes in general, the use of IVTT systems also offers unprecedented opportunities for combinatorial  
12  
13 approaches to exploring the functional impact of cofactor substitutions.  
14  
15  
16  
17  
18  
19  
20  
21  
22  
23  
24  
25  
26  
27  
28  
29  
30  
31  
32  
33  
34  
35  
36  
37  
38  
39  
40  
41  
42  
43  
44  
45  
46  
47  
48  
49  
50  
51  
52  
53  
54  
55  
56  
57  
58  
59  
60

1  
2  
3 **ASSOCIATED CONTENT**  
4

5 **Supporting Information.** Additional details on materials, methods, and data. This material is available  
6  
7 free of charge via the Internet at <http://pubs.acs.org>.  
8  
9

10  
11 **AUTHOR INFORMATION**  
12

13  
14 **Corresponding Author**  
15

16 \* Email: [sal2@emory.edu](mailto:sal2@emory.edu)  
17

18 **Notes**  
19

20 The authors declare no competing financial interests.  
21  
22  
23  
24

25 **ACKNOWLEDGMENT**  
26

27 The authors like to thank Drs. Roberto Orru and Dale Edmondson for their assistance with the stopped  
28 flow experiments and members of the Atlanta Flavin Group and the Lutz lab for helpful comments and  
29 suggestions. Support with PURExpress by Corinna Tuckey from New England Biolabs (Ipswich, MA) is  
30 acknowledged. This work was in part funded by the US National Science Foundation (CBET 0730312 &  
31 1159434).  
32  
33  
34  
35  
36  
37  
38  
39  
40  
41  
42  
43  
44  
45  
46  
47  
48  
49  
50  
51  
52  
53  
54  
55  
56  
57  
58  
59  
60

## REFERENCES

- (1) Lu, S. M.; Bolm, C. *Chemistry* **2008**, *14*, 7513.
- (2) Taylor, C. J. S. N.; Jaekel, C. *Adv. Synth. Catal.* **2008**, *350*, 2708.
- (3) Martin, N. J. A.; List, B. *J. Am. Chem. Soc.* **2006**, *128*, 13368.
- (4) Tuttle, J. B.; Ouellet, S. G.; MacMillan, D. W. C. *J. Am. Chem. Soc.* **2006**, *128*, 12662.
- (5) Bornscheuer, U. T.; Huisman, G. W.; Kazlauskas, R. J.; Lutz, S.; Moore, J. C.; Robins, K. *Nature* **2012**, *485*, 185.
- (6) Nestl, B. M.; Nebel, B. A.; Hauer, B. *Curr. Opin. Chem. Biol.* **2011**, *15*, 187.
- (7) Wohlgemuth, R. *Curr. Opin. Biotechnol.* **2010**, *21*, 713.
- (8) Kawai, Y.; Inaba, Y.; Tokitoh, N. *Tetrahedron-Asymmetr.* **2001**, *12*, 309.
- (9) Kosjek, B.; Fleitz, F. J.; Dormer, P. G.; Kuethe, J. T.; Devine, P. N. *Tetrahedron-Asymmetr.* **2008**, *19*, 1403.
- (10) Hall, M.; Stueckler, C.; Hauer, B.; Stuermer, R.; Friedrich, T.; Breuer, M.; Kroutil, W.; Faber, K. *Eur. J. Org. Chem.* **2008**, *9*, 1511.
- (11) Swiderska, M. A.; Stewart, J. D. *J. Mol. Catal. B-Enzym* **2006**, *42*, 52.
- (12) Adalbjornsson, B. V.; Toogood, H. S.; Fryszkowska, A.; Pudney, C. R.; Jowitt, T. A.; Leys, D.; Scrutton, N. S. *Chembiochem* **2010**, *11*, 197.
- (13) Toogood, H. S.; Fryszkowska, A.; Hare, V.; Fisher, K.; Roujeinikova, A.; Leys, D.; Gardiner, J. M.; Stephens, G. M.; Scrutton, N. S. *Adv. Synth. Catal.* **2008**, *350*, 2789.
- (14) Toogood, H. S.; Gardiner, J. M.; Scrutton, N. S. *Chemcatchem* **2010**, *2*, 892.
- (15) Stueckler, C.; Mueller, N. J.; Winkler, C. K.; Glueck, S. M.; Gruber, K.; Steinkellner, G.; Faber, K. *Dalton T.* **2010**, *39*, 8472.
- (16) Hall, M.; Stueckler, C.; Ehammer, H.; Pointner, E.; Oberdorfer, G.; Gruber, K.; Hauer, B.; Stuermer, R.; Kroutil, W.; Macheroux, P.; Faber, K. *Adv. Synth. Catal.* **2008**, *350*, 411.
- (17) Winkler, C. K.; Tasnadi, G.; Clay, D.; Hall, M.; Faber, K. *J. Biotechnol.* **2012**, *162*, 381.

- 1  
2  
3  
4  
5  
6  
7  
8  
9  
10  
11  
12  
13  
14  
15  
16  
17  
18  
19  
20  
21  
22  
23  
24  
25  
26  
27  
28  
29  
30  
31  
32  
33  
34  
35  
36  
37  
38  
39  
40  
41  
42  
43  
44  
45  
46  
47  
48  
49  
50  
51  
52  
53  
54  
55  
56  
57  
58  
59  
60
- (18) Schittmayer, M.; Glieder, A.; Uhl, M. K.; Winkler, A.; Zach, S.; Schrittwieser, J. H.; Kroutil, W.; Macheroux, P.; Gruber, K.; Kambourakis, S.; Rozzell, J. D.; Winkler, M. *Adv. Synth. Catal.* **2011**, *353*, 268.
- (19) Pompeu, Y. A.; Sullivan, B.; Walton, A. Z.; Stewart, J. D. *Adv. Synth. Catal.* **2012**, *354*, 1949.
- (20) Hulley, M. E.; Toogood, H. S.; Fryszkowska, A.; Mansell, D.; Stephens, G. M.; Gardiner, J. M.; Scrutton, N. S. *Chembiochem* **2010**, *11*, 2433.
- (21) Toogood, H. S.; Fryszkowska, A.; Hulley, M.; Sakuma, M.; Mansell, D.; Stephens, G. M.; Gardiner, J. M.; Scrutton, N. S. *Chembiochem* **2011**, *12*, 738.
- (22) Bougioukou, D. J.; Kille, S.; Taglieber, A.; Reetz, M. T. *Adv. Synth. Catal.* **2009**, *351*, 3287.
- (23) Padhi, S. K.; Bougioukou, D. J.; Stewart, J. D. *J. Am. Chem. Soc.* **2009**, *131*, 3271.
- (24) Hall, M.; Bommarius, A. S. *Chem. Rev.* **2011**, *111*, 4088.
- (25) Reich, S.; Hoeffken, H. W.; Rosche, B.; Nestl, B. M.; Hauer, B. *Chembiochem* **2012**, *13*, 2400.
- (26) Brown, B. J.; Hyun, J. W.; Duvvuri, S.; Karplus, P. A.; Massey, V. *J. Biol. Chem.* **2002**, *277*, 2138.
- (27) Vaz, A. D. N.; Chakraborty, S.; Massey, V. *Biochemistry* **1995**, *34*, 4246.
- (28) Niino, Y. S.; Chakraborty, S.; Brown, B. J.; Massey, V. *J. Biol. Chem.* **1995**, *270*, 1983.
- (29) Massey, V.; Schopfer, L. M. *J. Biol. Chem.* **1986**, *261*, 1215.
- (30) Fox, K. M.; Karplus, P. A. *Structure* **1994**, *2*, 1089.
- (31) Karplus, P. A.; Fox, K. M.; Massey, V. *FASEB J.* **1995**, *9*, 1518.
- (32) Yu, Y.; Lutz, S. *Trends Biotechnol.* **2011**, *29*, 18.
- (33) Qian, Z.; Lutz, S. *J. Am. Chem. Soc.* **2005**, *127*, 13466.
- (34) Qian, Z.; Fields, C. J.; Lutz, S. *Chembiochem* **2007**, *8*, 1989.
- (35) Qian, Z.; Horton, J. R.; Cheng, X.; Lutz, S. *J. Mol. Biol.* **2009**, *393*, 191.
- (36) Whitehead, T. A.; Bergeron, L. M.; Clark, D. S. *Protein Eng. Des. Sel.* **2009**, *22*, 607.
- (37) Stephen, P.; Tseng, K. L.; Liu, Y. N.; Lyu, P. C. *Chem. Commun. (Camb)*. **2012**, *48*, 2612.
- (38) Guntas, G.; Kanwar, M.; Ostermeier, M. *PLoS ONE* **2012**, *7*, e35998.

- 1  
2  
3 (39) Ueda, T.; Shimizu, Y.; Inoue, A.; Tomari, Y.; Suzuki, T.; Yokogawa, T.; Nishikawa, K. *Nature*  
4  
5 *Biotechnol.* **2001**, *19*, 751.  
6  
7  
8 (40) *Protein Generation Using a Reconstituted System* in Protein Engineering Handbook; Ying, B.  
9 W.; Ueda, T., Eds.; Wiley-VCH: Weinheim, 2009; Vol. 2.  
10  
11 (41) Brown, B. J.; Deng, Z.; Karplus, P. A.; Massey, V. *J. Biol. Chem.* **1998**, *273*, 32753.  
12  
13 (42) Reitinger, S.; Yu, Y.; Wicki, J.; Ludwiczek, M.; D'Angelo, I.; Baturin, S.; Okon, M.; Strynadka,  
14 N. C.; Lutz, S.; Withers, S. G.; McIntosh, L. P. *Biochemistry* **2010**, *49*, 2464.  
15  
16  
17 (43) Abramovitz, A. S.; Massey, V. *J. Biol. Chem.* **1976**, *251*, 5327.  
18  
19 (44) Stuermer, R.; Hauer, B.; Hall, M.; Faber, K. *Curr. Opin. Chem. Biol.* **2007**, *11*, 203.  
20  
21 (45) Wada, M.; Yoshizumi, A.; Noda, Y.; Kataoka, M.; Shimizu, S.; Takagi, H.; Nakamori, S. *Appl.*  
22 *Environ. Microbiol.* **2003**, *69*, 933.  
23  
24  
25 (46) Kataoka, M.; Kotaka, A.; Hasegawa, A.; Wada, M.; Yoshizumi, A.; Nakamori, S.; Shimizu, S.  
26 *Biosci. Biotechnol. Biochem.* **2002**, *66*, 2651.  
27  
28  
29 (47) Fryszkowska, A.; Toogood, H.; Sakuma, M.; Gardiner, J. M.; Stephens, G. M.; Scrutton, N. S.  
30 *Adv. Synth. Catal.* **2009**, *351*, 2976.  
31  
32  
33 (48) Ay, J.; Hahn, M.; Decanniere, K.; Piotukh, K.; Borriss, R.; Heinemann, U. *Proteins* **1998**, *30*,  
34 155.  
35  
36  
37 (49) Chu, V.; Freitag, S.; Le Trong, I.; Stenkamp, R. E.; Stayton, P. S. *Protein Sci.* **1998**, *7*, 848.  
38  
39  
40 (50) Manjasetty, B. A.; Hennecke, J.; Glockshuber, R.; Heinemann, U. *Acta Crystallogr. D Biol.*  
41 *Crystallogr.* **2004**, *60*, 304.  
42  
43  
44 (51) Pieper, U.; Hayakawa, K.; Li, Z.; Herzberg, O. *Biochemistry* **1997**, *36*, 8767.  
45  
46  
47 (52) Matthews, R. G.; Massey, V.; Sweeley, C. C. *J. Biol. Chem.* **1975**, *250*, 9294.  
48  
49  
50 (53) van den Heuvel, R. H.; van den Berg, W. A.; Rovida, S.; van Berkel, W. J. *J. Biol. Chem.* **2004**,  
51 *279*, 33492.  
52  
53  
54  
55  
56  
57  
58  
59  
60

**FIGURE LEGENDS**

**Figure 1.** Assembly of cpOYE library via whole-gene synthesis. Two copies of truncated *oye1* (marked in red and blue) were prepared that lack the three native C-terminal amino acids and the Start/Stop codons. The two genes were assembled in tandem and connected by a 9-nucleotide sequence encoding the -Gly-Thr-Ser- linker. PCR amplification with site-specific primers and the tandem repeat as template yielded individual members of the CP library and reintroduced Start/Stop codons, as well as flanking restriction sites for the subsequent cloning into pET-14b. Correct gene constructs (cpOYE#) were confirmed by DNA sequencing, sorted and stored as purified plasmids in microtiterplates.

**Figure 2.** Primary screening data of cpOYE library for ene-reductase activity on A.) ketoisophorone (**1**) to levodione (*R*-**2**), B.) cinnamaldehyde (**3**) to dihydrocinnamaldehyde (**4**), and C.) carvone (*S*-**5**) to dihydrocarvone (*cis*-(*1R,4S*)-**6**). Whole-gene synthesis created a native cpOYE library with perfect distribution (red lines in inner circle). Catalytic activity of library members for each substrate was measured by semi-quantitative assay and is reflected in the length of the green lines. Wild-type activity is indicated by the grey-shaded area. The outer-most circle marks the secondary structure elements (shades of blue) and active site residues (yellow stars) of OYE1 (399 amino acid residues). For all three substrates, four sectors (I - IV) in the protein sequence with activity equal or better than wild-type were identified.

**Figure 3.** Schematic of OYE1 structure (based on PDB access code 1K03<sup>26</sup>). The FMN cofactor is shown in blue sticks while the substrate-binding site is occupied by *p*-hydroxybenzaldehyde (dotted cloud). The location of permutation sites which resulted in catalytic improvements are highlighted in red (sectors I), orange (sectors II), yellow (sectors III) and green (sectors IV), respectively.

**Figure 4.** Rapid reaction kinetics for wild type OYE1 and cpOYE303. A.) Complete reaction cycle for OYE with rate constants for the reductive and oxidative half reactions of OYE1 (green) and cpOYE303

1  
2  
3 (red). B.) Changes in flavin spectra for wild type and cp variant during reductive half reaction. The  
4 characteristic absorption band of FMN<sub>ox</sub> near 460 nm (blue diamonds) disappears upon conversion to  
5 FMN<sub>red</sub> (orange circles). For OYE1, global fit analysis indicates formation of a short-lived intermediate  
6 with a slightly red-shifted maximum near 460 nm (black squares) corresponding to the charge-transfer  
7 complex in E•FMN<sub>ox</sub>•NADPH. For cpOYE303, no such intermediate was detectable. C.) Observed rate  
8 for the reductive half reaction as a function of [NADPH] based on the disappearance of the FMN<sub>ox</sub>  
9 absorption band. Given experimental restraints to [NADPH] >50 μM, data analysis was limited to  
10 determination of maximum rates ( $k_{red}$ ). D.) Flavin reoxidation ( $k_{ox}$ ) upon rapid mixing of E•FMN<sub>red</sub> with **1**  
11 (0.5 mM) under anaerobic conditions followed single-exponential kinetics. Experimental data are shown  
12 for the overall and initial (insert) oxidative half reaction catalyzed by wild type OYE1 (grey) and  
13 cpOYE303 (black). Curve fits are displayed as red lines.  
14  
15  
16  
17  
18  
19  
20  
21  
22  
23  
24  
25  
26  
27  
28  
29  
30  
31  
32  
33  
34  
35  
36  
37  
38  
39  
40  
41  
42  
43  
44  
45  
46  
47  
48  
49  
50  
51  
52  
53  
54  
55  
56  
57  
58  
59  
60

SCHEME 1

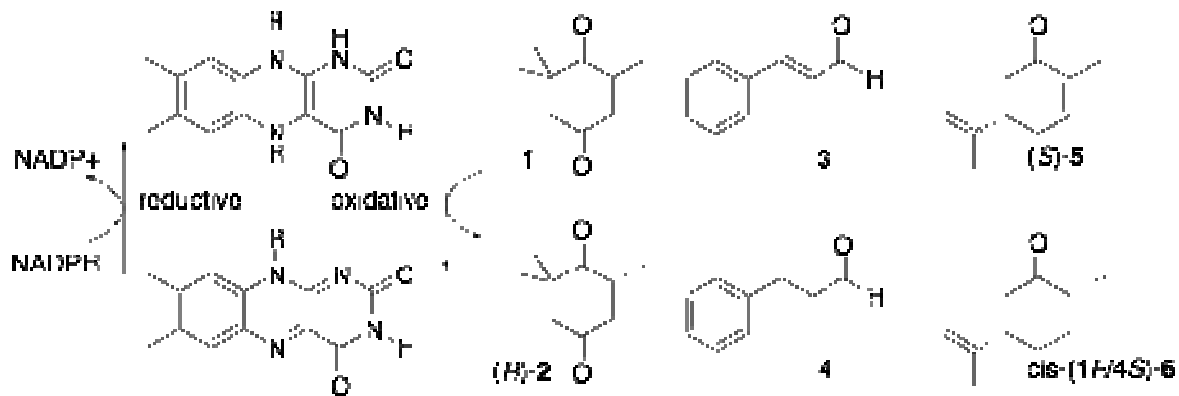


TABLE 1

**Table 1.** Comparison of biocatalytic rates for reduction of ketoisophorone (**1**), cinnamaldehyde (**3**), and S-carvone (**5**).

Variant	IVT( <b>1</b> ) <sup>[a]</sup>	EA( <b>1</b> ) <sup>[b]</sup> (min <sup>-1</sup> )	EA( <b>3</b> ) <sup>[c]</sup> (min <sup>-1</sup> )	EA( <b>5</b> ) <sup>[c]</sup> (min <sup>-1</sup> )
OYE1	1x	6.5 (1x)	53 (1x)	1.9 (1x)
cpOYE146	1.3x	19 (3x)	60 (1.1x)	1.4 (0.8x)
cpOYE154	0.8x	12.2 (2x)	83 (1.5x)	6 (3x)
cpOYE160	1.6x	10.1 (1.6x)	85 (1.6)	9.5 (5x)
cpOYE257	1x	13 (2x)	44 (0.8x)	5.7 (3x)
cpOYE260	2x	25.4 (4x)	113 (2x)	7.7 (4x)
cpOYE291	3.2x	36 (6x)	21 (0.4x)	3.4 (1.8x)
cpOYE303	5.3x	122 (19x)	24 (0.4x)	22.5 (12x)
cpOYE306	4.2x	47.2 (7x)	42 (0.8x)	23.6 (13x)
cpOYE378	0.7x	nd	57 (1x)	5.9 (3x)

<sup>[a]</sup> Fold activity change in based on GC analysis. Conversion rate (fold-change) of regular enzyme activity (EA) measurements via <sup>[b]</sup> GC or <sup>[c]</sup> UV analysis. Standard error for IVT data  $\pm 100\%$ ; EA data  $\pm 10\%$ . nd = not determined.

TABLE 2

Table 2. Spectral property changes upon inhibitor binding.

Variant	$K_D(\mu\text{M})^{[a]}$	$\lambda_{\text{max}}(\text{CT}; \text{nm})$ $(\epsilon = \text{M}^{-1}\text{cm}^{-1})$	$(\epsilon \lambda_{\text{max}}(\text{FMN}; \text{nm}))$ $(\epsilon = \text{M}^{-1}\text{cm}^{-1})$	$E^{\circ\prime}$ (mV) <sup>[b]</sup>
OYE1	$1.6 \pm 0.4$	578 (4335)	460 (10600)	-207
cpOYE154	$1.0 \pm 0.3$	582 (3753)	457 (12784)	-196
cpOYE160	$0.6 \pm 0.2$	572 (2971)	462 (11913)	-210
cpOYE257	$1.9 \pm 0.7$	566 (2485)	463 (11341)	-214
cpOYE260	$1.1 \pm 0.4$	580 (2973)	460 (11979)	-200
cpOYE291	$4.0 \pm 1.0$	564 (2956)	464 (12260)	-216
cpOYE303	$1.9 \pm 0.2$	569 (2685)	463 (13147)	-212
cpOYE306	$2.9 \pm 0.9$	565 (2756)	458 (10774)	-215
cpOYE378	$2.3 \pm 0.9$	578 (3702)	458 (12224)	-207

<sup>[a]</sup> Dissociation constant for *p*-hydroxybenzaldehyde. <sup>[b]</sup>  $E^{\circ\prime}$ -values were estimated based on correlation of  $\lambda_{\text{max}}(\text{CT})$  band with FMN  $E^{\circ\prime}$ -values.<sup>43</sup> Standard error:  $\pm 5$  mV.

FIGURE 1

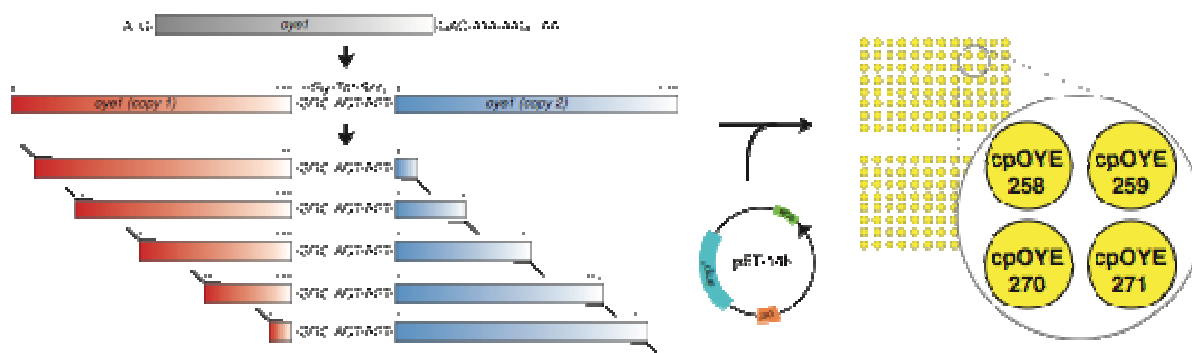


FIGURE 2

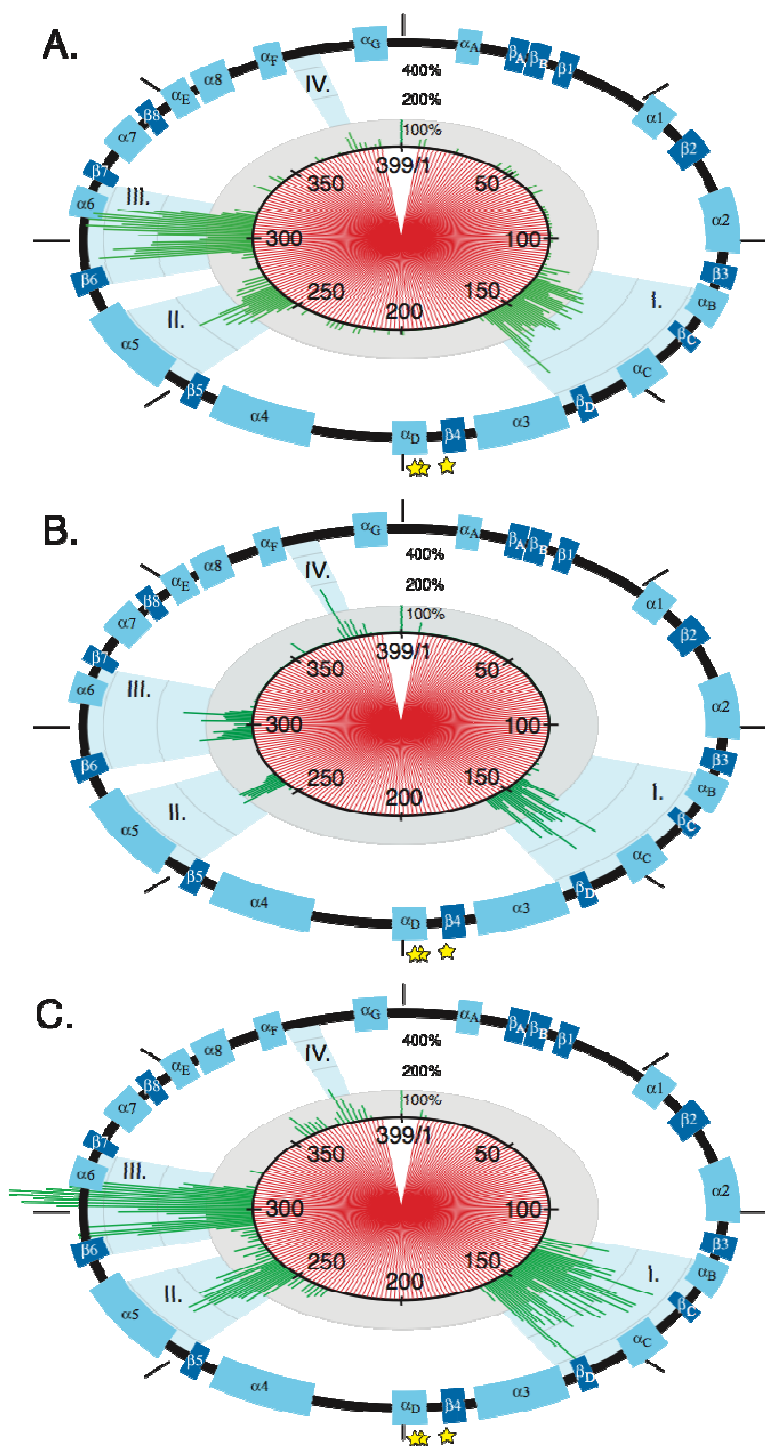


FIGURE 3

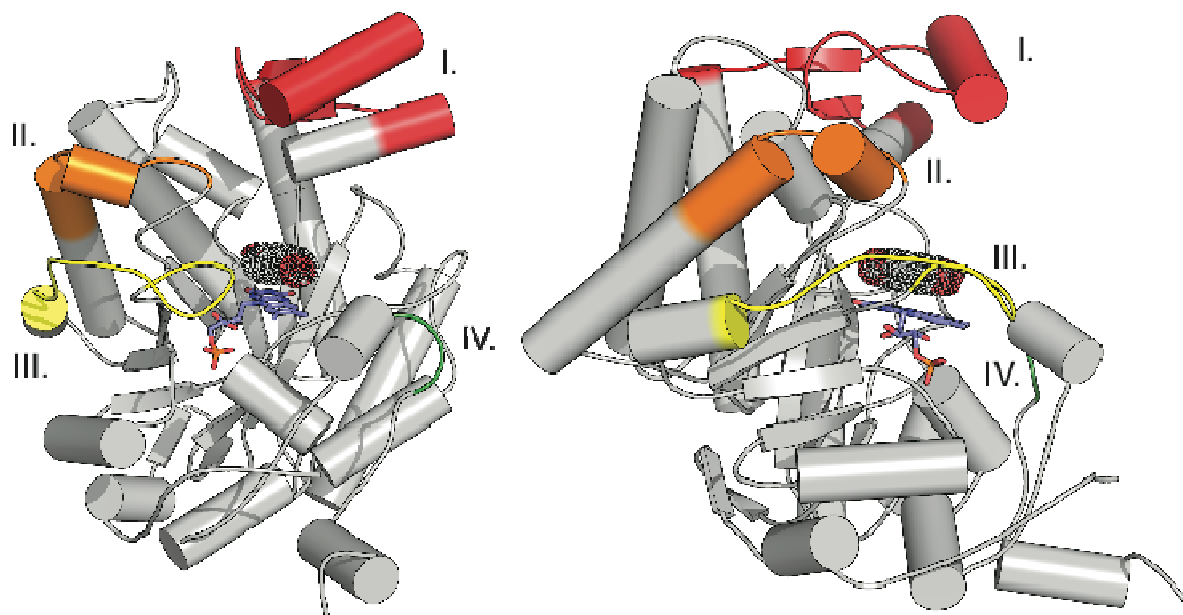
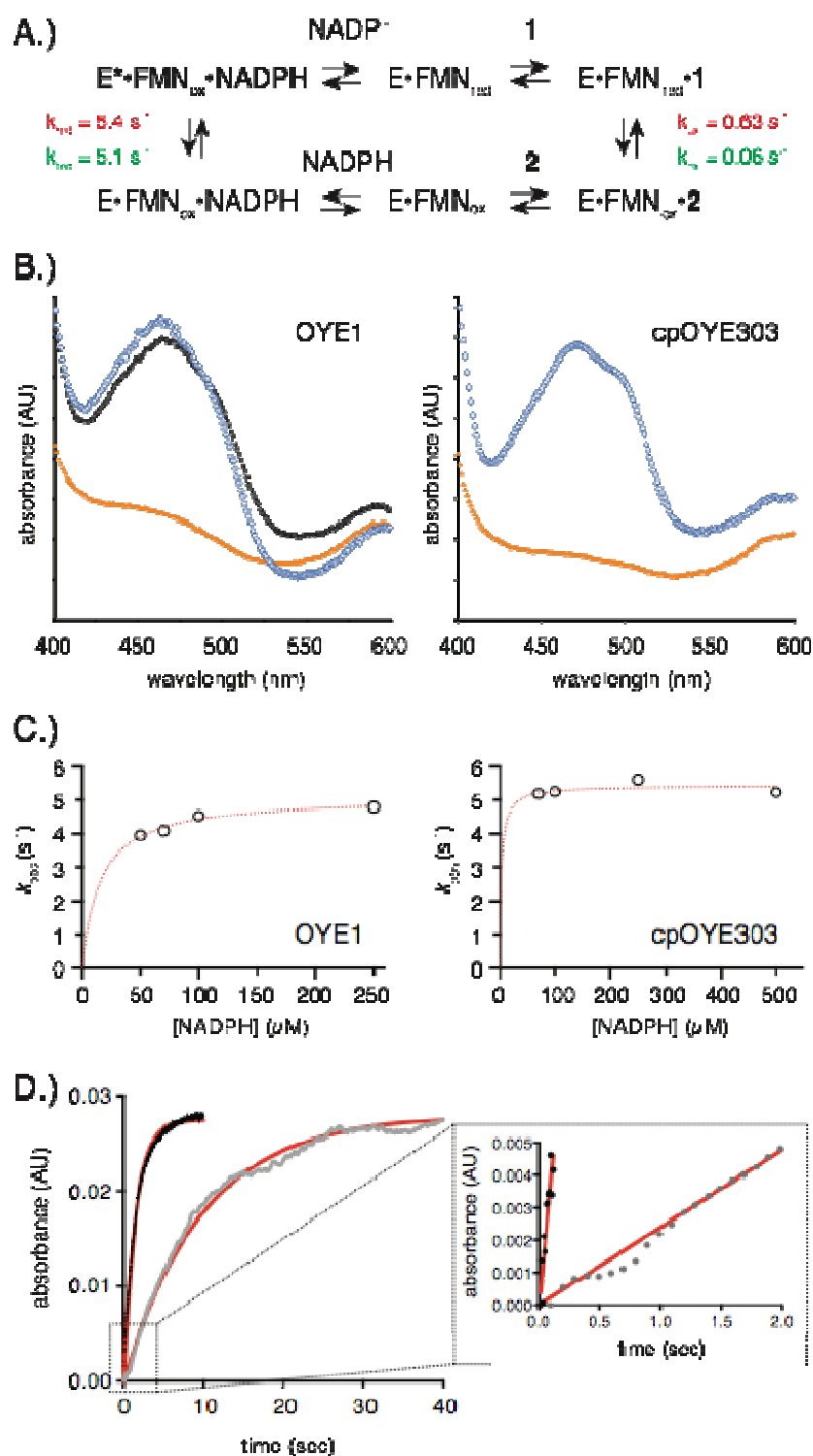
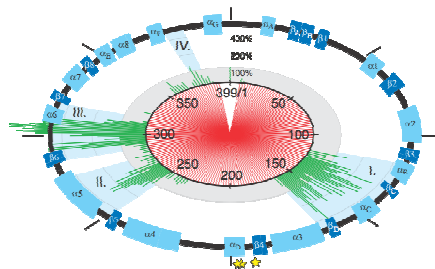
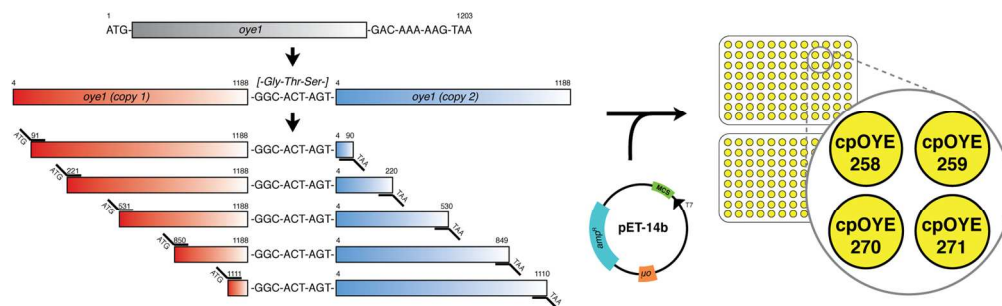


FIGURE 4

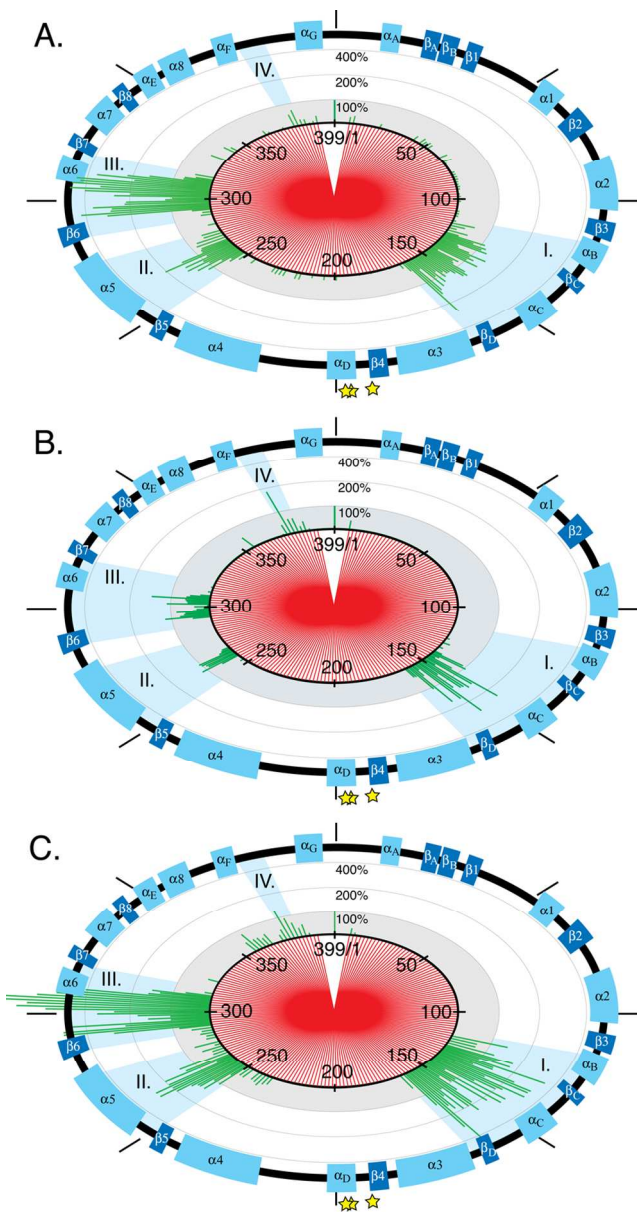


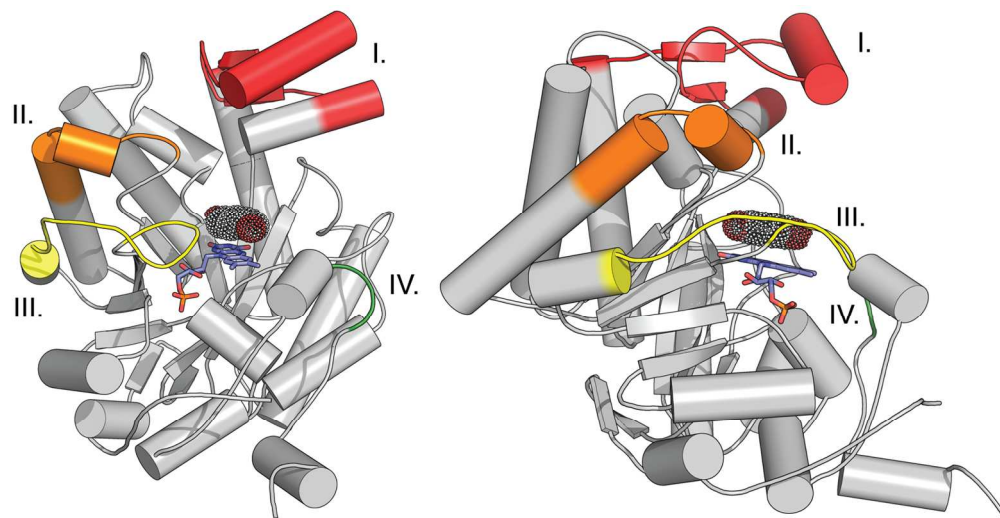
## TABLE OF CONTENTS GRAPHIC



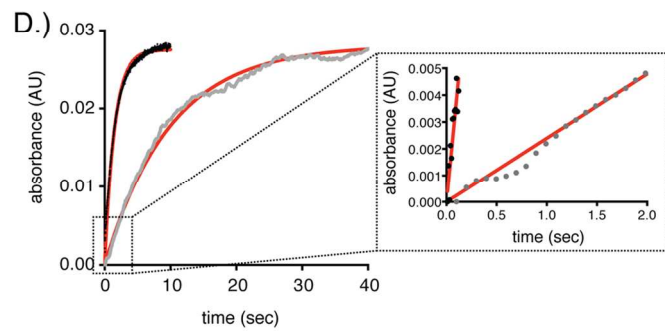
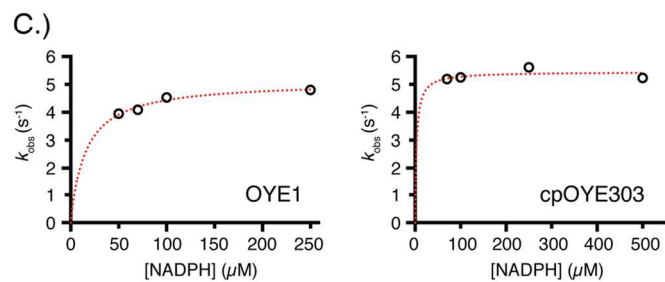
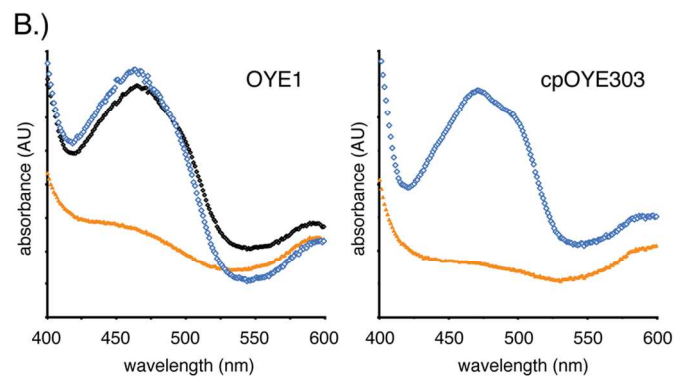
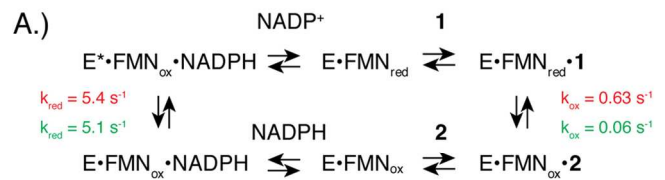


152x45mm (300 x 300 DPI)

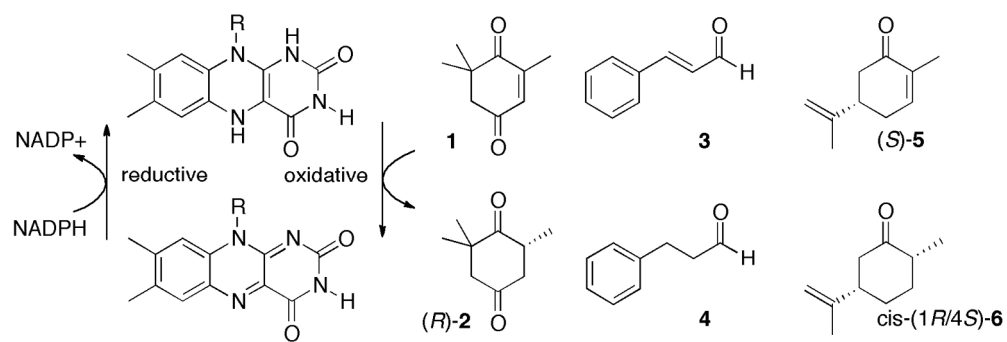




152x79mm (300 x 300 DPI)



83x149mm (300 x 300 DPI)



164x55mm (300 x 300 DPI)